

# The Influence of Piezoceramic Stack Location on Nonlinear Behavior of Langevin Transducers

Andrew Mathieson, Andrea Cardoni, Niccolò Cerisola, and Margaret Lucas

**Abstract**—Power ultrasonic applications such as cutting, welding, and sonochemistry often use Langevin transducers to generate power ultrasound. Traditionally, it has been proposed that the piezoceramic stack of a Langevin transducer should be located in the nodal plane of the longitudinal mode of vibration, ensuring that the piezoceramic elements are positioned under a uniform stress during transducer operation, maximizing element efficiency and minimizing piezoceramic aging. However, this general design rule is often partially broken during the design phase if features such as a support flange or multiple piezoceramic stacks are incorporated into the transducer architecture. Meanwhile, it has also been well documented in the literature that power ultrasonic devices driven at high excitation levels exhibit nonlinear behaviors similar to those observed in Duffing-type systems, such as resonant frequency shifts, the jump phenomenon, and hysteretic regions. This study investigates three Langevin transducers with different piezoceramic stack locations by characterizing their linear and nonlinear vibrational responses to understand how the stack location influences nonlinear behavior.

## I. INTRODUCTION

LANGDEVIN transducers, which are also known as stack or sandwich transducers, are often used in power ultrasonic applications to generate high intensity ultrasound by driving them close to resonance at high excitation levels. They are generally constructed from four fundamental components; back mass, front mass, piezoceramic stack, and a bolt that holds the transducer together under a compressive pre-load [1]. The traditional configuration of Langevin transducers locates the piezoceramic stack at the node of the longitudinal mode of vibration so that piezoceramic element efficiency can be maximized and their aging can be minimized [2]–[4]. However, to enable the transducer to be supported with minimal damping it is often more advantageous to locate a support flange in the longitudinal nodal plane, thus shifting the stack out of the plane [5], [6].

More recently, the development of multi-frequency power ultrasonic transducers for applications in sonochemistry [4] and the advance of multi-mode ultrasonic transducers and ultrasonic motors [7], [8] has resulted in transducer architectures that contain multiple sets of piezoceramic stacks. Multi-frequency transducers can contain two piezoceramic stacks which are located at different positions within the transducer and, through independently driving these stacks, allow the transducer to be driven at two distinct resonant frequencies [4], [9]. Multi-mode transducers can also contain multiple piezoceramic stacks, although these are often individually poled and driven simultaneously to couple longitudinal and flexural vibrations or longitudinal and torsional vibrations. The piezoceramic stack which is poled to induce longitudinal vibration is generally located at or close to the nodal plane of the longitudinal mode whereas the stack that induces flexural or torsional vibrations is positioned to maximize these responses [10]. Therefore, the architecture of these multi-frequency and multi-mode transducers provides the opportunity for one of the piezoceramic stacks to be positioned in a location of significant longitudinal motion.

The influence that piezoceramic stack location has on transducer performance was first reported during the 1970s [5], [6], [11], as well as more recently [2]–[4]. These studies investigated transducer properties such as mechanical quality factor,  $Q_m$ , effective electro-mechanical coefficient,  $k_{\text{eff}}$ , and resonant frequency through numerical and experimental methods. Although it was reported [11] that these properties differed based on excitation level, the studies did not investigate whether stack position influenced nonlinear responses or drive stability. This current study therefore investigates whether stack location has a significant influence on the linear and nonlinear vibration behaviors of Langevin transducers, where nonlinearities are characterized by shifts in resonant frequency, the jump phenomenon, hysteretic widths, and multi-modal responses.

## II. TRANSDUCERS

Three half-wavelength Langevin transducers, each with a different piezoceramic stack location, were manufactured, Fig. 1, and are referred to as TI, TII, and TIII. The stack, held under a pre-stress via an internal stud, contains piezoceramic rings with properties of PZT4 with

Manuscript received September 18, 2012; accepted March 11, 2013. This work has been funded by the Engineering and Physical Sciences Research Council (EPSRC) grant EP/E025811/1, with Mectron S.p.A, Carasco, Genoa, as a project partner.

A. Mathieson and M. Lucas are with the School of Engineering, University of Glasgow, Glasgow, UK (e-mail: andrew.mathieson@glasgow.ac.uk).

A. Cardoni is with Pusions SL, Arganda del Rey, Spain.

N. Cerisola is with Mectron S.p.A, Carasco, GE, Italy.

DOI <http://dx.doi.org/10.1109/TUFFC.2013.2675>

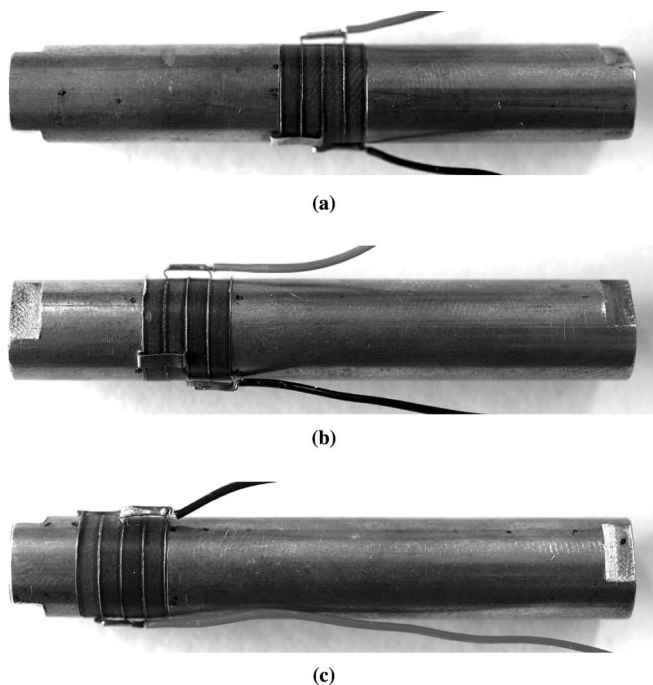


Fig. 1. Transducer configurations: (a) TI, (b) TII, and (c) TIII.

a diameter of 10 mm. Four elements were employed in the stack to replicate piezoceramic volumes typical of high-power ultrasonic transducers of similar diameters. TI consists of a centrally positioned piezoceramic stack, located in the nodal plane of the first longitudinal mode of vibration, and has two brass end masses of equal length. TII and TIII contain end masses of length ratios 1/3 to 3/4 and 1/8 to 7/8, respectively, and hence the piezoceramic stack is positioned away from the nodal plane.

### III. MEASUREMENT TECHNIQUES

#### A. Resonant Frequency and Mode Shape Extraction

Experimental modal analysis (EMA) was used to detect all modes of vibration in the frequency range of 0 to 94 kHz. The transducers were excited via a random excitation signal at low power by a function generator built into the data acquisition hardware (Quattro, Data Physics Corp., San Jose, CA), and then amplified through a power amplifier (RMX 4050HD, QSC Audio Products LLC, Costa Mesa, CA). Velocity responses were measured over a grid of points located on the surface of the transducers using a 3-D laser Doppler vibrometer (CLV-3D, Polytec GmbH, Waldbronn, Germany), and the acquired frequency response functions, with a resolution of 1.6 Hz, were recorded using Signal Calc ACE data acquisition software (Data Physics Corp.). The frequency response function data were then imported in to modal analysis software (ME'ScopeVES, Vibrant Technology Inc., Scotts Valley, CA), where the acquired measurements underwent curve

fitting to generate a parametric model of the FRF experimental data. From the parametric model, the modes in the frequency span of the FRF data were determined and the modal parameters (modal frequency and mode shape) were identified. To visualize the mode shapes, the modal data were attributed to the associated grid points on a 3-D model, representing the geometry of the transducers, which could be animated to illustrate the oscillation.

#### B. Harmonic Characterization

Bi-directional frequency sweeps were used to excite the transducers close to the frequency of the first longitudinal mode. Previous studies have reported that piezoceramic properties such as  $k_{\text{eff}}$ ,  $Q_m$ , and dielectric loss factor,  $\delta$ , which are all indicators of piezoceramic or transducer performance, were shown to be dependent on electric field strength, vibrational stress, and temperature, whereas the elastic compliance,  $s^E$ , dielectric constant,  $\epsilon^T$ , and piezoelectric constant,  $d$ , have also shown to be temperature- and vibrational-stress-dependent [12]–[17]. Therefore, to investigate the influence of piezoceramic stack location, rather than the influence of elevated piezoceramic stack temperature, on the vibration response of the transducers, the transducers were excited under constant voltage conditions with a burst-sine signal at each frequency increment of the sweeps [16]. Each burst-sine signal was applied for a fixed number of 4000 cycles, which was long enough for steady-state vibration to be achieved but short enough to minimize temperature increases in the stack. To further remove temperature effects, a time delay of 1 s between successive bursts was incorporated for excitation levels in the range 1 to 10  $V_{\text{rms}}$ , and a delay of 10 s for excitation levels in the range 10 to 50  $V_{\text{rms}}$ , which was sufficient to dissipate any heat build-up. To observe small changes in the vibrational response of the transducers at excitation levels in the 1 to 10  $V_{\text{rms}}$  range, the frequency step between successive frequency bursts was set at 1 Hz. For excitation levels in the 10 to 50  $V_{\text{rms}}$  range, the frequency step was set at 2 Hz to ensure that each sweep could be accurately controlled.

For these measurements, the transducers were excited by a signal generated by a function generator (3322A, Agilent Technologies Inc., Santa Clara, CA) which was amplified through a power amplifier (QSC RMX 4050HD) and the vibration velocity response of each transducer was measured at its free end (free end of the short end mass for TII and TIII) using a 1-D laser Doppler vibrometer (CFV 055, Polytec GmbH) while the temperature of the piezoceramic stack was measured using an infrared sensor. Data acquisition hardware and interface (National Instruments Corp., Austin, TX) in conjunction with Labview software were used to coordinate the experimental protocol and data collection; the time-domain signals of current and voltage as well as the frequency spectrum of the velocity response were viewed on an oscilloscope (DPO 7054, Tektronix Inc., Beaverton, OR).

TABLE I. FREQUENCIES OF MODES OF VIBRATION MEASURED THROUGH EMA. B: BENDING MODE OF VIBRATION, L: LONGITUDINAL MODE OF VIBRATION, T: TORSIONAL MODE OF VIBRATION.

	B1	T1	B2	L1	B3	B4	L2	B5	B6	L3
TI	—	14970	19022	26864	32 484	45319	58134	61104	73867	80761
TII	8099	15460	19108	28216	—	—	55426	62827	76825	81496
TIII	8609	15463	19108	29295	33169	47584	55626	—	74492	83452

#### IV. RESULTS AND DISCUSSION

##### A. Linear Regime of Vibration: Modal Responses

The modes of vibration extracted from an EMA are indicated next to their corresponding resonant frequency on the measured frequency response functions, see Fig. 2; all extracted resonant frequencies are given in Table I. It can be observed in Fig. 2 that, as expected, the responses of longitudinal modes of vibration are generally stronger than the responses of bending and torsional modes of vibration.

However, it is also evident that the location of the piezoceramic stack influences the response of different modes of vibration. It can be observed that the first bending mode of vibration is detected in the responses of TII and TIII,

despite being absent in the response of TI. Meanwhile, Figs. 2(b) and 2(c) illustrate that the response of the second longitudinal mode of vibration is strong in TII and TIII. However, the weak response of the mode exhibited in the response of TI, Fig. 2(a), indicates that the response of longitudinal modes of vibration are also affected by piezoceramic stack location. Contour plots depicting the longitudinal modes of vibration of TI, TII and TIII are presented in Fig. 3(a). It can be interpreted from studying Figs. 2 and 3(a) that the response of longitudinal modes of vibration are strong in transducers in which the piezoceramic stack is located at or close to the nodal plane. However, when the piezoceramic stack is located at an antinode, as in the second longitudinal mode of vibration of TI, the response of the mode is weak. Similarly, the first bending mode is only detected in the traces of TII and TIII, Fig. 2. In both TII and TIII, the piezoceramic stack lies in close proximity to a nodal plane, whereas in TI, the piezoceramic stack lies at an antinode. Furthermore, the third and fourth bending modes are not detected in TII, and the fifth bending mode is not detected in TIII. As the piezoceramic stack would be located close to the antinode of these modes in the respective transducers, this indicates that modes of vibration exhibit stronger responses if the piezoceramic stack is located at or close to the mode's nodal plane and weaker responses if it is located at the antinode.

This observation could be utilized to control vibrational behavior through the design of ultrasonic devices, particularly slender full wavelength devices that exhibit coupling between longitudinal and bending modes of vibration. Such modal coupling is often detrimental to device performance and can result in premature failure. Locating the piezoceramic stack close to the antinode of unwanted modes reduces the influence of these modes on the vibrational response, allowing the effect on device performance to be minimized.

##### B. Linear Regime of Vibration: Electromechanical Properties

The  $k_{\text{eff}}$  values for the transducers, at the first longitudinal mode, were calculated from

$$k_{\text{eff}} = \sqrt{(f_p^2 - f_s^2)/f_s^2}, \quad (1)$$

using measurements of the serial resonant frequency,  $f_s$ , and parallel resonant frequency,  $f_p$ , recorded from an impedance analyzer (4294A, Agilent Technologies Inc.). These values were found to be 0.351, 0.295 and 0.207 for

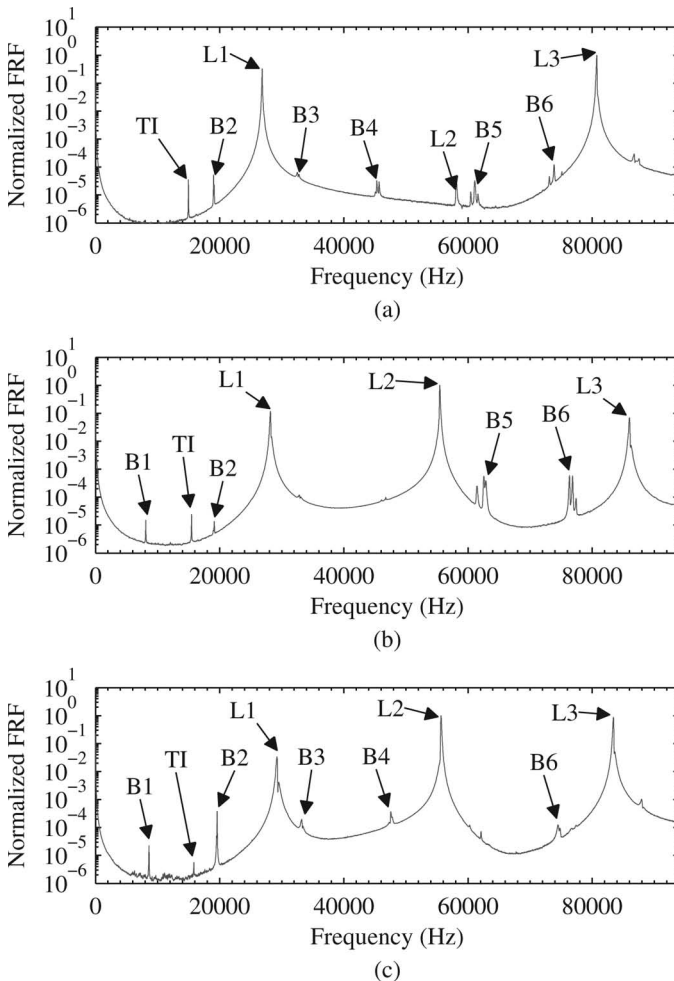


Fig. 2. Curve-fitted FRFs: (a) TI, (b) TII, and (c) TIII. L = longitudinal, B = bending, T = torsional.

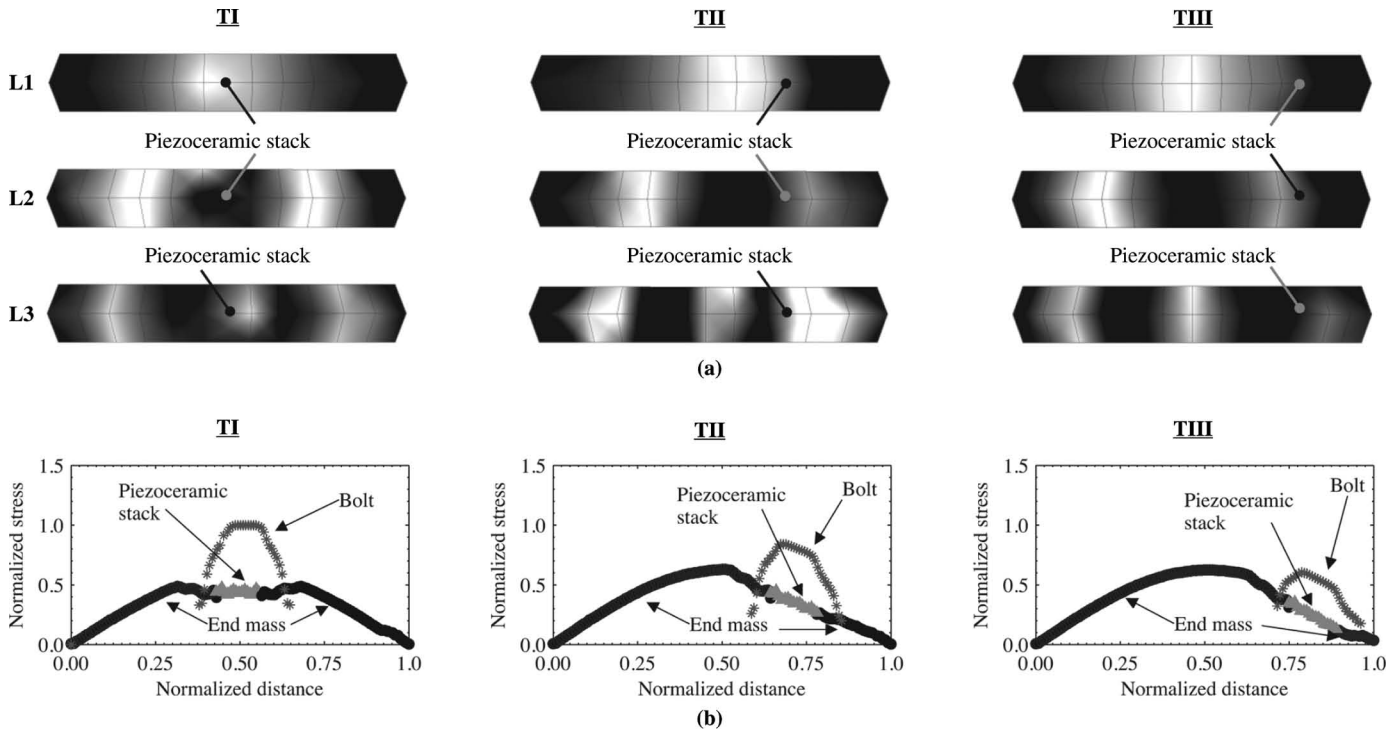


Fig. 3. (a) Undeformed normalized displacement contour maps depicting longitudinal mode shapes (light regions are nodal, dark regions are antinodal). (b) Normalized vibrational stress predicted through center of bolt, mean radius of transducer end mass and piezoceramic elements for first longitudinal mode of vibration.

TI, TII and TIII, respectively. Fig. 4 presents the first longitudinal mode response to bi-directional frequency sweeps at an excitation level of  $1 V_{\text{rms}}$ , from which the  $Q_m$  of each transducer was calculated. TI exhibited the highest  $Q_m$  value, 255; the values for TII and TIII were 187 and 112. As  $k_{\text{eff}}$  represents the efficiency of the transducer to convert electrical energy to strain, and  $Q_m$  is governed by the transducer damping, these can be used to indicate the potential transducer efficiency and performance. For low excitation levels, it was found that TI exhibited the highest values of  $k_{\text{eff}}$  and  $Q_m$ , suggesting that optimal transducer performance at low excitation levels occur when the piezoceramic stack is located at the nodal plane and thus reiterating the previous finding that longitudinal modes of vibration are better excited when the piezoceramic stack is located at the node.

The resonant frequencies of the first longitudinal mode for TI, TII and TIII, identified through bi-directional frequency sweeps at an excitation level of  $1 V_{\text{rms}}$ , Fig. 4, were measured at 26576, 28031, and 29111 Hz. These show good correlation with the frequencies of the first longitudinal mode acquired through EMA, Table I. The percentage difference in measured frequency between the two methods was found to be 1.07%, 0.66%, and 0.53% for TI, TII, and TIII, respectively. The most significant factor influencing these very small percentage differences in frequencies is the different excitation signals; a random signal was used to excite the transducers during the EMA, whereas a sinusoidal signal was utilized during the bi-directional sweep.

### C. Nonlinear Regime of Vibration: Duffing-Type System

The vibration displacement amplitude responses of the transducers, at seven excitation levels between  $1 V_{\text{rms}}$  and  $50 V_{\text{rms}}$ , are presented in Fig. 5. Although at low levels of excitation the response of the transducers is linear (Fig. 4), indicated by the symmetric response curves, at elevated excitation levels the asymmetric responses are typical of a dynamic system exhibiting the stiffness softening effect observed in Duffing-type systems. The equation of motion of a general Duffing oscillator system is

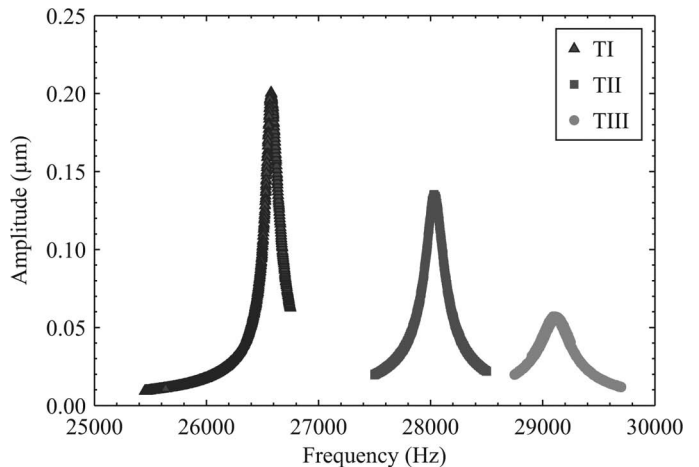


Fig. 4. Vibrational response transducer in the region of the first longitudinal mode at  $1 V_{\text{rms}}$ .

$$\ddot{u} + 2\beta\omega_0\dot{u} + \omega_0^2u + \gamma u^3 = q \cos(\Omega t), \quad (2)$$

where  $\omega_0$  is the undamped linear natural frequency of the system;  $\beta$  is the damping ratio;  $\ddot{u}$ ,  $\dot{u}$ , and  $u$  are generalized acceleration, velocity, and displacement terms, respective-

ly; and  $\gamma u^3$  is a Duffing or nonlinear (cubic) stiffness term. The cubic term determines the direction of the leaning of the frequency response curve for increasing excitation levels. Stiffness softening occurs when  $\gamma$  is negative and causes the curve to bend to the left, indicating a lowering in resonant frequency. A consequence of high stiffness softening is the manifestation of the jump phenomenon and the appearance of a significant hysteresis region in the measured response, Fig. 5(a). The jump phenomenon is characterized by a discontinuity in the frequency response curve caused by a sudden increase or jump in amplitude of vibration between two frequencies and can occur during both upward and downward frequency sweep measurements.

A hysteresis region is formed during a bi-directional frequency sweep, and is the result of the difference between the resonant frequency found during the upward sweep and that found during the downward sweep. If the transducer is driven at a frequency that corresponds with an amplitude jump or within the frequency range of the hysteresis region, the transducer has the possibility of operating at either a high or a low amplitude of vibration. This is therefore an unstable region for transducer operation.

Fig. 6 plots the shift in resonant frequency against amplitude of vibration of the transducer and it can be seen that the shift in resonant frequency increases with amplitude of vibration. It is evident from comparison of the transducers at low amplitudes of vibration ( $<1.0 \mu\text{m}$ ) that TI and TII exhibit a similar shift in resonant frequency, whereas at higher vibrational amplitudes ( $>1.0 \mu\text{m}$ ) TI exhibits the largest resonant frequency shift of the three transducers investigated. Meanwhile, TIII exhibits the smallest shift in resonant frequency over the measured vibration amplitude range. The jump phenomenon was also observed in the amplitude responses of all transducer configurations. TI exhibits a jump at the lowest excitation voltage,  $5 V_{\text{rms}}$ , and lowest amplitude of vibration,  $1.21 \mu\text{m}$ , TII and TIII exhibit jumps at higher voltages,  $20 V_{\text{rms}}$  and  $40 V_{\text{rms}}$ , and higher vibrational amplitudes,  $3.41 \mu\text{m}$  and  $3.50 \mu\text{m}$ , respectively.

Duffing-like behavior has been documented in piezoceramic elements and Langevin transducers in previous studies [14]–[18]. Although in the general solution the cubic term is responsible for Duffing-like behavior, in power ultrasonic devices it is known to stem from several sources [19]. Such behavior observed in the responses of piezoceramic elements (kept at constant temperature) has been attributed to the elastic compliance changing proportionally with the square of vibrational stress when excited above a vibrational threshold [12]. Geometrical features, such as threaded joints without sufficient preloading, have also been observed to induce significant resonant frequency shifts and hysteresis widths [19].

From Fig. 6, it is clear that piezoceramic stack location also influences these behaviors. At elevated vibrational amplitudes, it is clear that the closer the piezoceramic stack is to the nodal plane, the larger the shift in resonant

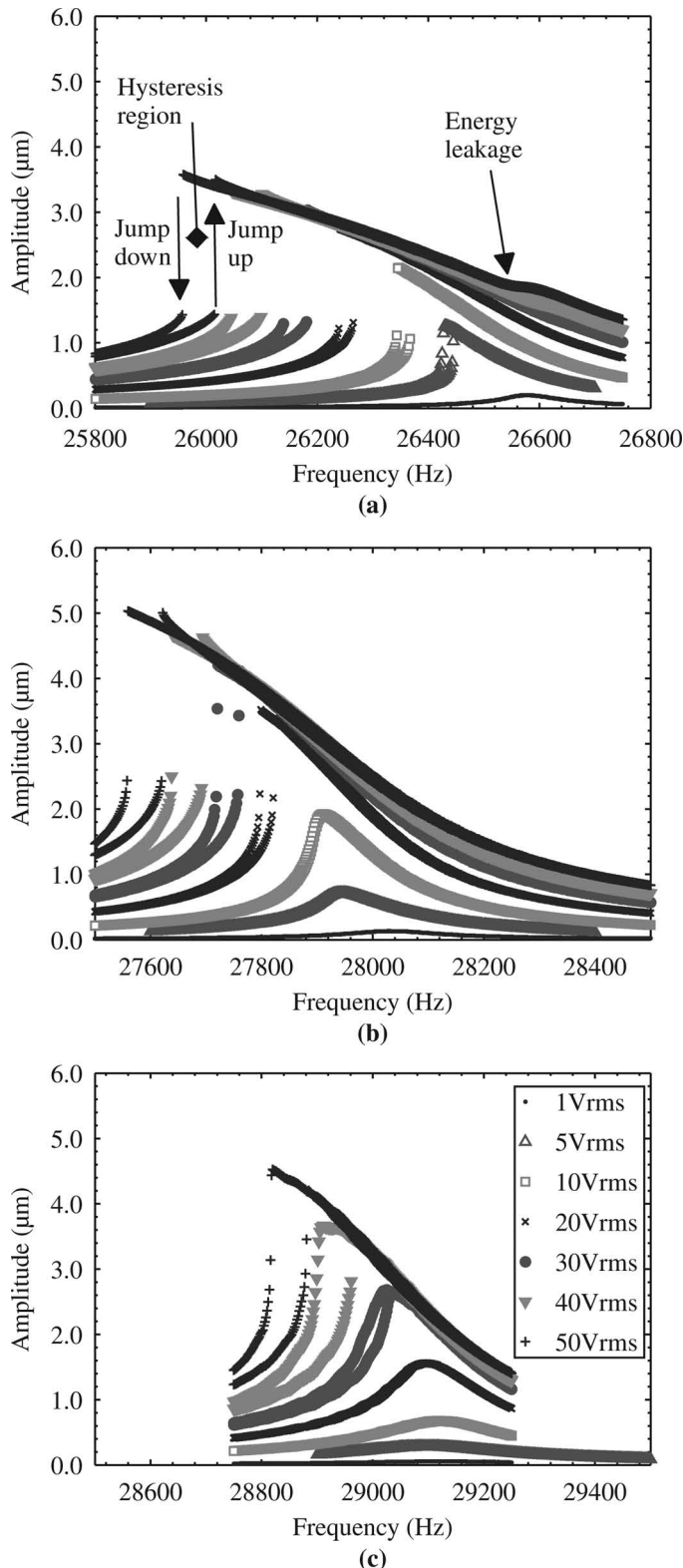


Fig. 5. Vibrational response at excitation levels from 1 to  $50 V_{\text{rms}}$ : (a) TI, (b) TII, and (c) TIII.

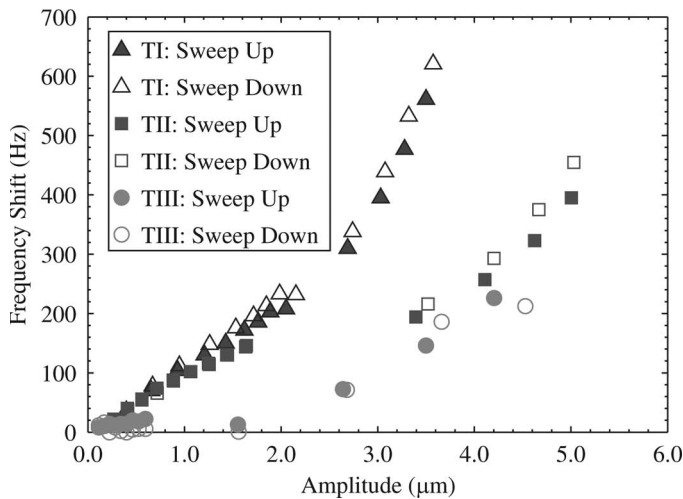


Fig. 6. Resonant frequency shift against vibrational response of the transducers.

frequency and the lower the vibrational amplitude before the jump phenomenon manifests in the response curve. Fig. 3(b) presents normalized vibrational stress along the length of the transducers, predicted using finite element analysis (Abaqus, Dassault Systèmes S.A., Vélizy-Villacoublay, France), for the first longitudinal mode of vibration. It is clear from Figs. 3(a) and 3(b) that when TI is driven at the first longitudinal mode, the piezoceramic stack is located in a region of higher vibrational stress than the piezoceramic stack in TII or TIII. It can also be observed from Fig. 3(b) that when TIII is driven at the first longitudinal mode, the piezoceramic stack is located in a region of lower vibrational stress. Therefore, it is evident that locating the piezoceramic stack away from the nodal plane could reduce the influence of resonant frequency shift and the jump phenomenon on transducer behavior.

Fig. 7 plots the frequency width of the hysteresis region against the amplitude of vibration at which hysteresis regions are first observed. Below an amplitude of vibration of  $1.0 \mu\text{m}$ , hysteresis regions do not appear in the responses of TI and TII, whereas TIII exhibits a hysteretic width of 14 Hz at  $1.0 \mu\text{m}$ . However, at a higher amplitude of vibration,  $3.5 \mu\text{m}$ , TI exhibits the largest width (58 Hz) and TII exhibits the smallest (24 Hz). Although these measurements indicate that the higher the vibration amplitude is, the greater is the frequency width of the hysteresis region, it can also be observed that the frequency widths at  $3.5 \mu\text{m}$  exhibited by TI and TIII are similar. This indicates that piezoceramic stack location does not influence this behavior as significantly as it does for the other nonlinear behaviors, resonant frequency shift and the jump phenomenon. However, studies of power ultrasonic devices have reported that the width of the hysteretic region can be significantly influenced by elevated piezoceramic element temperature and joint preloading in ultrasonic devices [19]. The temperature variation on the surface of the piezoceramic stack in this study was mea-

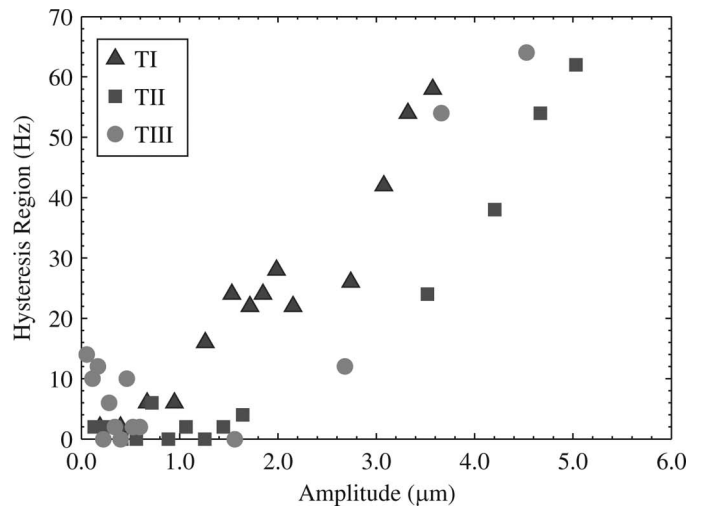


Fig. 7. Width of hysteresis region against vibrational response of the transducers.

sured to be  $3.01^\circ\text{C}$ ,  $2.98^\circ\text{C}$ , and  $2.07^\circ\text{C}$ , during the bi-directional frequency sweeps between 1 and  $50 \text{ V}_{\text{rms}}$ , for TI, TII, and TIII respectively. The increase in piezoceramic stack temperature was therefore not large enough to influence piezoceramic properties such as  $Q_m$  and  $s^E$ . This also indicates that the burst length and the time delay between successive bursts were sufficient to minimize the influence of elevated piezoceramic temperatures on the nonlinear behaviors. It can also be assumed that joint preloading in the piezoceramic stack did not significantly vary for the different piezoceramic stack locations.

These findings can also influence the design of transducers. The width of the hysteretic region is a measure of the size of the unstable region within which frequency tracking of the transducer is ineffective. However, where there is a small stiffness softening leading to a resonant frequency shift but without a hysteresis region, then it is still possible to track resonance. In this study, the location of the piezoceramic stack does not significantly affect the size of the unstable region but does affect the level of stiffness softening, and thus leads to a conclusion that a transducer with a centrally located piezoceramic stack is worst.

#### D. Nonlinear Regime of Vibration: Autoparametric Response

Autoparametric vibration has been well documented in dynamic systems [20], including ultrasonic cutting devices [21], and occurs when the driven mode of vibration parametrically excites an undesired mode or modes of vibration. For autoparametric vibration to exist, a dynamic system must be excited at resonance,  $\omega_1$ , above a vibrational threshold, while one or more other resonant frequencies of the system are excited due to a simple integer (or near integer) relationship such as;  $\omega_1 \approx 2\omega_2$ ,  $\omega_1 \approx \omega_2 + 2\omega_3$ , or  $\omega_1 \approx 1/2\omega_2$ .

An indicator of autoparametric vibration is exhibited in the vibrational response of TI, Fig. 5(a). A shallow dip is

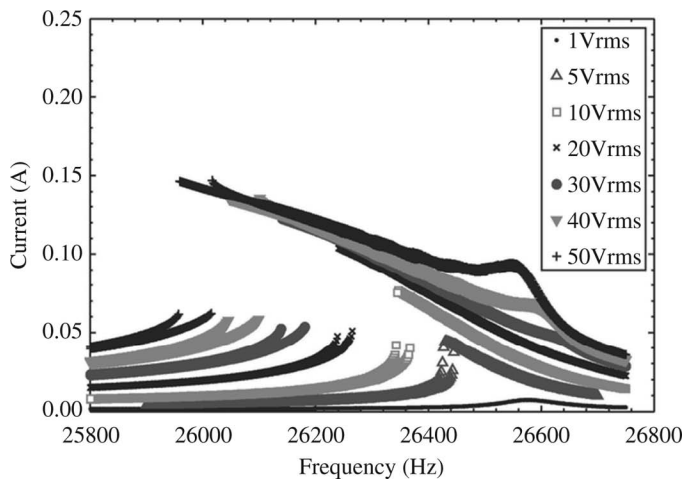


Fig. 8. Current drawn by TI in the frequency region of the first longitudinal mode.

present in the response (between 26 490 Hz and 26 660 Hz) above an excitation level of 30  $V_{\text{rms}}$ . It can be observed from Fig. 8 that there is an increase in current drawn above the same excitation level and in the same frequency range. An increase in the current drawn by the transducer should be accompanied by an increase in vibrational amplitude. However the reduction in vibrational amplitude indicates that energy is leaking from the first longitudinal mode of vibration to another mode. The measured spectral response of TI, excited at 50  $V_{\text{rms}}$  and 26 520 Hz (Fig. 9), illustrates the response of the driving or fundamental frequency of vibration,  $\omega_1$ , the first harmonic,  $\omega_2$ , and second harmonic,  $\omega_3$ . Although the response of  $\omega_2$  is relatively weak, the strong response of  $\omega_3$  suggests that this is the frequency of the autoparametrically excited mode. Fig. 10 presents the vibrational response of  $\omega_3$  while TI was excited close the first longitudinal mode. It is clear that a resonant peak lies within the frequency range of 79 470 to 79 980 Hz. Fig. 9 illustrates that a frequency ratio of 3:1 exists between the fundamental and autoparametric response. Although the same frequency ratio exists between the first and third longitudinal modes of vibration, the resonance peak observed in Fig. 10 does not directly correspond with the resonant frequency of the third longitudinal mode of vibration measured during EMA, Table I. However, it can also be observed that the mode of vibration excited in Fig. 10 exhibits stiffness softening. Therefore if the third longitudinal mode frequency shifted to a lower frequency, it will retain a necessary simple frequency ratio of 3:1 with the first longitudinal mode for this mode to be excited autoparametrically.

From these findings, asymmetry in the transducer helps to reduce the number of unwanted modes strongly excited in the transducer and also removes many of the simple mathematical relationships between the fundamental longitudinal mode frequency and its harmonics. In this case, locating the piezoceramic stack away from the nodal plane reduces the likelihood of autoparametric responses.

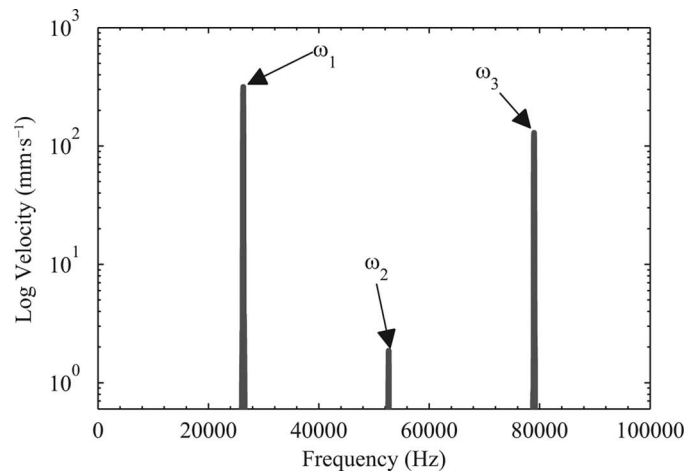


Fig. 9. TI spectral response, captured from oscilloscope. Excitation: 50  $V_{\text{rms}}$ ,  $\omega_1 = 26520$  Hz,  $\omega_2 = 52646$  Hz,  $\omega_3 = 79509$  Hz.

## V. CONCLUSIONS

The linear and nonlinear behavior of three Langevin transducers with different piezoceramic stack locations has been discussed. Measurements recorded in the linear regime of vibration response indicate that modes of vibration are more responsively excited when the piezoceramic stack is located at the nodal plane of the mode of vibration. Practically, this finding could be utilized in the control of vibrational behavior in ultrasonic devices, especially modal coupling that is often prominent in slender full wavelength power ultrasonic devices. Meanwhile, measurements taken at elevated amplitudes of vibration indicate that the location of the piezoceramic stack can influence two Duffing-like behaviors; resonant frequency shifts and the jump phenomenon. However, these measurements also reveal that piezoceramic stack location has less influence on the frequency widths of the hysteresis regions. Finally, an autoparametric response was exhibited in the frequency response of TI. The combination of EMA and harmonic characterization at elevated vibrational am-

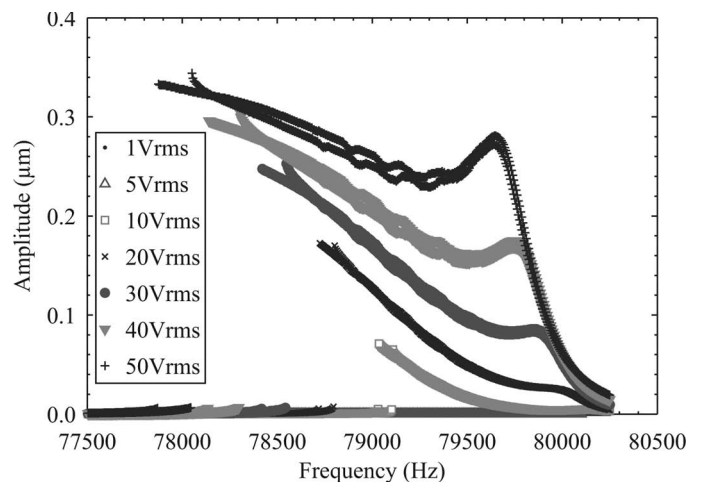


Fig. 10. TI vibrational response of  $\omega_3$  while driven in first longitudinal mode at  $\omega_1$ .

plitudes allowed the excitation of the third longitudinal mode to be identified as the autoparametric response. The findings demonstrate that location of the piezoceramic stack in high-power ultrasonic transducers must be carefully considered against the nonlinear behaviors as well as the more conventional performance indicators extracted from responses in the linear vibration regime.

#### ACKNOWLEDGMENTS

The Power Ultrasonics Group of the Consejo Superior de las Investigaciones Científicas (CSIC), Madrid, is acknowledged for allowing access to their laboratory facilities.

#### REFERENCES

- [1] H. Minchenko, "Electromechanical transducer," U.S. Patent 3396285, Aug. 6, 1968.
- [2] L. Shuyu and Z. Fucheng, "Study of vibrational characteristics for piezoelectric sandwich ultrasonic transducers," *Ultrasonics*, vol. 32, no. 1, pp. 39–42, 1994.
- [3] L. Shuyu, "Optimization of the performance of the sandwich piezoelectric ultrasonic transducer," *J. Acoust. Soc. Am.*, vol. 115, no. 1, pp. 182–186, 2004.
- [4] L. Shuyu, "Analysis of multifrequency Langevin composite ultrasonic transducers," *IEEE Trans. Ultrason. Ferroelectr. Freq. Control*, vol. 56, no. 9, pp. 1990–1998, 2009.
- [5] A. Shoh, "Sonic transducer," U.S. Patent 3524085, Aug. 11, 1970.
- [6] E. A. Neppiras, "The pre-stressed piezoelectric sandwich transducer," in *Int. Ultrasonics Conf. Proc.*, 1973, pp. 295–302.
- [7] Y. Tomikawa, K. Adachi, M. Aoyagi, T. Sagae, and T. Takano, "Some constructions and characteristics of rod-type piezoelectric ultrasonic motors using longitudinal and torsional vibrations," *IEEE Trans. Ultrason. Ferroelectr. Freq. Control*, vol. 39, no. 5, pp. 600–608, 1992.
- [8] K. Uchino and J. Giniewicz, *Micromechatronics*. New York, NY: Marcel Dekker, 2003.
- [9] L. Shuyu and X. Chunlong, "Analysis of the sandwich ultrasonic transducer with two sets of piezoelectric elements," *Smart Mater. Struct.*, vol. 17, no. 6, art. no. 065008, 2008.
- [10] Y. Watanabe, Y. Tsuda, and E. Mori, "A longitudinal-flexural complex-mode ultrasonic high-power transducer system with one-dimensional construction," *Jpn. J. Appl. Phys.*, vol. 32, no. 5B, pp. 2430–2434, 1993.
- [11] R. LeMaster and K. Graff, "Influence of ceramic location on high power transducer performance," in *Int. Ultrasonics Symp. Proc.*, 1978, pp. 296–299.
- [12] S. Takahashi, Y. Sasaki, M. Umeda, and K. Nakamura, S. Ueha, "Nonlinear behavior in piezoelectric ceramic transducers," in *IEEE Int. Symp. Applications of Ferroelectrics*, 2000, vol. 1, pp. 11–16.
- [13] M. Umeda, K. Nakamura, and S. Ueha, "Effects of vibration stress and temperature on the characteristics of piezoelectric ceramics under high vibration amplitude levels measured by electrical transient method," *Jpn. J. Appl. Phys.*, vol. 38, no. 9B, pp. 5581–5585, 1999.
- [14] M. Umeda, K. Nakamura, S. Takahashi, and S. Ueha, "An analysis of jumping and dropping phenomena of piezoelectric transducers using the electrical equivalent circuit constants at high vibration amplitude levels," *Jpn. J. Appl. Phys.*, vol. 39, no. 9B, pp. 5623–5628, 2000.
- [15] J. F. Blackburn and M. G. Cain, "Nonlinear piezoelectric resonance: A theoretically rigorous approach to constant I-V measurements," *J. Appl. Phys.*, vol. 100, no. 11, art. no. 114101, 2006.
- [16] A. Albareda, R. Perez, J. Casals, J. Garcia, and D. Ochoa, "Optimization of elastic nonlinear behavior measurements of ceramic piezoelectric resonators with burst excitation," *IEEE Trans. Ultrason. Ferroelectr. Freq. Control*, vol. 54, no. 10, pp. 2175–2188, 2007.
- [17] D. Guyomar, B. Ducharme, and G. Sebald, "High nonlinearities in Langevin transducer: A comprehensive model," *Ultrasonics*, vol. 51, no. 8, pp. 1006–1013, 2011.
- [18] N. Aurelle, D. Guyomar, C. Richard, P. Gonnard, and L. Eyraud, "Nonlinear behavior of an ultrasonic transducer," *Ultrasonics*, vol. 34, no. 2–5, pp. 187–191, 1996.
- [19] A. Mathieson, "Nonlinear characterisation of power ultrasonic devices used in bone surgery," Ph.D. thesis, School of Engineering, University of Glasgow, Glasgow, UK, 2012.
- [20] M. Cartmell, *Introduction to Linear, Parametric and Nonlinear Vibrations*. London, UK: Chapman and Hall, 1991.
- [21] A. Cardoni, F. Lim, M. Lucas, and M. Cartmell, "Characterising modal interactions in an ultrasonic cutting system," in *Forum Acusticum*, Seville, Spain, 2002, art. no. ULT-02–003-IP.



**Andrew Mathieson** was born in Glasgow, Scotland, in 1984. He obtained an M.Eng. degree in mechanical engineering in 2007 and then a Ph.D. degree in 2012, both from the University of Glasgow. Currently, Andrew is working as a researcher in power ultrasonics at the University of Glasgow, where his research interests include the application of power ultrasonics to medical and industrial applications.



**Andrea Cardoni** was born in Camogli, Italy, in 1974. He obtained a B.Eng. degree from the University of Glasgow in 1998, an M.Eng. degree from the University of Genoa in 1999, and a Ph.D. degree from the University of Glasgow in 2003, all in mechanical engineering. He then worked as a lecturer at the University of Glasgow, with research interests in power ultrasonic technology applied to industrial, medical, and space applications. Dr. Cardoni is now the Technical director of Pusonics SL, of Arganda del Rey, Madrid, Spain.



**Niccolò Cerisola** was born in Chiavari, Italy, in 1980. He obtained a biomedical engineering degree from the University of Genoa in 2005. Since 2006, Niccolò has worked in the research and development department of the dental and surgical device manufacturer Mectron S.p.A., Carasco (Genoa), Italy.



**Margaret Lucas** was born in Edinburgh, Scotland, in 1961. She obtained a B.Sc.(Eng.) degree in mechanical engineering from the University of Aberdeen, followed by a Ph.D. degree in mechanical engineering at Loughborough University. She was a lecturer in dynamics at Loughborough University before moving to the University of Glasgow in 1996, where she is currently Professor of Ultrasonics. Her research interests are in industrial and medical applications of power ultrasonics.